ACS Chemical Neuroscience

Article

Circular dichroism spectroscopy identifies the #-adrenoceptor agonist salbutamol as a direct inhibitor of tau filament formation *in vitro*.

David J Townsend, Barbora Mala, Eleri Hughes, Rohanah Hussain, Giuliano Siligardi, Nigel J Fullwood, and David A. Middleton

ACS Chem. Neurosci., **Just Accepted Manuscript** • DOI: 10.1021/acschemneuro.0c00154 • Publication Date (Web): 10 Jun 2020

Circular dichroism spectroscopy identifies the β-adrenoceptor agonist salbutamol as a direct inhibitor of tau filament formation *in vitro*.

David J. Townsend*, Barbora Mala, Eleri Hughes, Rohanah Hussain, Giuliano Siligardi, Nigel J. Fullwood, & David A. Middleton.

Corresponding Author: *d.townsend1@lancaster.ac.uk

Abstract

Potential drug treatments for Alzheimer's disease (AD) may be found by identifying compounds that block the assembly of the microtubule-associated protein tau into neurofibrillar tangles associated with neuron destabilisation and cell death. Here, a small library of structurally diverse compounds was screened *in vitro* for the ability to inhibit tau aggregation, using high-throughput synchrotron radiation circular dichroism (HT-SRCD) as a novel tool to monitor the structural changes in the protein as it assembles into filaments. The catecholamine epinephrine was found to be the most effective tau aggregation inhibitor of all 88 compounds screened. Subsequently, we tested chemically-similar phenolamine drugs from the β-adrenergic receptor (βAR) agonist class, using conventional circular dichroism spectroscopy, thioflavin T fluorescence and transmission electron microscopy. Two compounds, salbutamol and dobutamine, used widely in the treatment of respiratory and cardiovascular disease, impede the aggregation of tau *in vitro*. Dobutamine reduces both the rate and yield of tau filament formation over 24 hours, although it has little effect on the structural transition of tau into β-sheet structures over 24 hours. Salbutamol also reduces the yield and rate of filament formation, and additionally inhibits tau's structural change into β-sheet rich aggregates. Salbutamol has a good safety profile and a half-life that facilitates permeation through the blood brain barrier and could represent an expediated approach to developing AD therapeutics. These results provide the motivation for *in vivo* evaluation of pre-existing β-adrenergic receptor agonists as a potential therapy for AD through the reduction of tau deposition in AD.

Key-words

Alzheimer's, tau, amyloid, β-adrenoceptor, salbutamol, dobutamine.

1. Introduction

Alzheimer's disease (AD) is classed by the world health organisation as a global health priority affecting 47 million people worldwide. With an increasingly aging population this figure is expected to triple to over 130 million cases by the year 2050, with an economic burden of $0.8T.[1,2] The increase in the incidence of AD is compounded by the lack of a significant breakthrough in drug therapies in the past 40 years[3] and no successful disease modifying treatment since its discovery in 1907.[4] Currently, only four drugs have been approved for use, all of which target the cholinergic or glutaminergic signalling pathways to reduce AD symptoms. None of these provides disease modifying therapeutic treatments.[5]

AD is characterised pathologically by the deposition of amyloid-β (Aβ) and tau proteins in the brain as insoluble amyloid fibrils and neurofibrillar tangles (NFT), respectively. In the tau hypothesis, tau, a collection of 6 alternatively spliced protein products of the MAPT gene,[6] undergoes hyperphosphorylation by glycogen synthase kinase enzymes.[7,8] Tau proteins normally associate with microtubules providing strength, polarity and support for neurons, but phosphorylation leads to its dissociation from the microtubules and the subsequent formation of NFT.[9] This step, which leads to neuron destabilisation and ultimately cell death[4,6–8] is thought to occur after the aggregation of Aβ and related inflammatory response in AD.[4,6,9] Although the amyloid and tau pathologies develop independently, there is evidence for a synergistic role of Aβ and tau in the development of AD, with evidence to support the oxidative damage caused by the early Aβ fibrils/oligomers leads to the hyperphosphorylation of tau.[4,7,8,10]

As well as its role in AD, tau NFT and neuropil threads are also associated with a number of other neurodegenerative diseases known collectively as tauopathies.[11] Recently, because of the failure of numerous Aβ targeted therapies to show any cognitive benefits for AD patients, even

where the therapies have been effective in clearing Aβ plaques,[12] attention has shifted towards tau. There are good reasons for believing tau is a more promising target for therapeutic intervention than Aβ. These include the observation that Aβ is not neurotoxic to tau-null cells.[13] In addition, reducing tau levels can eliminate behavioural deficits in transgenic mice with high Aβ.[14] It has been known for a long time that the distribution of tau pathology in AD correlates much better with the clinical severity of AD than the distribution of Aβ plaques.[15] Finally, the central role of tau in neurodegeneration is evident in diseases such as primary age-related tauopathy where Aβ plaques are absent.

One therapeutic approach for AD is to block or impair Aβ amyloid formation or tau NFT deposition. This is commonly done by stabilising the native monomeric proteins, by reducing the levels of amyloid precursors, or by increasing the clearance of the insoluble fibres or filaments.[5,7,8] In this context, much research has been carried out into the inhibition of amyloidosis by natural aromatic compounds,[16–24] including polyphenols from dietary substances that recognise the generic amyloid cross-β motif and alter the aggregation kinetics or restructure many amyloidogenic proteins into non-toxic species *in vitro*.[22–26] For example, the phenolic rings of polyphenol compounds interfere with the stacking of aromatic residues and hydroxyl groups, thereby destabilising the amyloid core and increasing its solubility.[27–29] A common first step toward identifying potential inhibitors is *in vitro* screening of compounds that reduce tau or Aβ self-assembly kinetics and yield. The amyloid-sensitive fluorescent dye thioflavin T (ThT) is a convenient tool that is amenable to high-throughput screening, but can report false positives when compounds compete for the same binding sites as the dye.[30] Circular dichroism (CD) spectroscopy is an alternative approach, which reports directly on the structural changes of the

protein as it undergoes aggregation and is therefore not prone to the ThT type of errors, but high-throughput analysis is more challenging.

Here we use high-throughput synchrotron radiation circular dichroism (HT-SRCD) as a novel primary screening platform to compare the inhibitory effects of a small library of drug-like compounds against tau filamentous assembly. Follow-up analysis of analogues of the most active compound, epinephrine, reveals the widely administered β_2-agonist salbutamol as a novel inhibitor of tau *in vitro*.

2. Results and Discussion

CD and ThT analysis of tau aggregation

The tau construct used for the duration of this work corresponds to residues 225-441 of the 4 microtubule binding repeat isoform of tau (Tau-4R), which has been shown to form microtubule assemblies *in vitro* with completion at around 4-6 hours.[31,32] Tau filament formation was followed initially using standard bench-top CD spectroscopy in the far-UV region. Upon amyloidosis, tau is expected to transition from a predominantly unordered native structure to a more ordered structure with a β-sheet core.[33] The CD spectrum of freshly-prepared, unaggregated tau exhibits a minimum around 200 nm (Figure 1A black), suggestive of a high unordered content or intrinsic disorder, as observed previously for tau.[33] Protein secondary structure estimation (SSE) form CD data using BeStSel algorithm[34,35] reveals the β-sheet content to be 42 ± 3.7 %, with the remaining structures consisting of turns (15 ± 1.5 %) as well as unordered conformation (33 ± 10.6 %). Induction of tau aggregation by the addition of heparin is accompanied by a progressive change in the spectra over 5 h (Figure 1A), coinciding with a slight increase in β-sheet content to 49 %. Little or no further change in the spectrum occurs between 5 h and 24 h, indicating that the fibrillisation process reaches conclusion around 5 h. The time-dependent change in CD, which does not occur in the absence of heparin, is characterised by an isodichroic point at around 205 nm. This is indicative of a single-phase transition from the initial secondary structure of un-aggregated tau, to a final structure adopted by the aggregated protein. Because of this, each spectrum acquired over the 5-hour period could be fitted by combinations of the initial (t = 0 h) and end-point (t = 5 h) spectra in different proportions in order to calculate the kinetics of the structural transformation. Hence, CD provides information on the aggregation kinetics and the structural transition of tau. The kinetics of the structural transformation

measured by CD matches the aggregation kinetics monitored in a separate experiment using ThT fluorescence, confirming that ThT binding occurs in parallel with the structural change (Figure 1B).

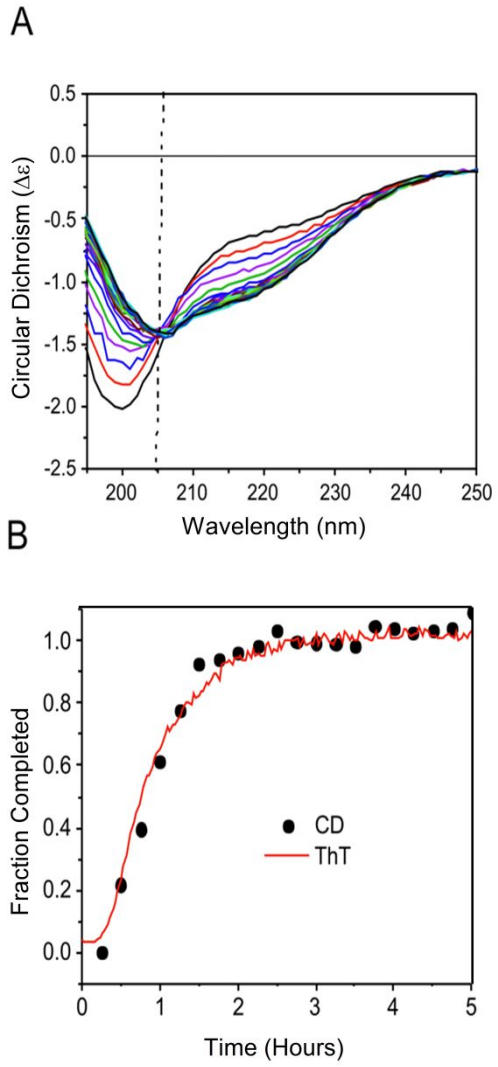

Figure 1. **A)** Far-UV CD spectra of tau protein under aggregation inducing conditions over 5 hours. **B**) Percentage completion of the structural transition over time (circles) overlaid with the time-dependent ThT fluorescence in the presence of 20 μM tau and 5 μM heparin.

High-throughput SRCD screening

HT-SRCD has been developed as a powerful new method for the rapid analysis of protein structures under a range of different conditions.[36] The highly collimated light beam enables samples to be measured using small aperture cells of low volume, which allows for measurements to be conducted on the centre of each well in a custom-designed 96-well plate without distortion effects, and the base area of the well can be scanned by moving a motorised X-Y stage in a rastering manner. A library of 88 drug and drug-like compounds, covering a broad range of chemical structures and indications, was selected from the LOPAC^{1280} series (Supporting Information Table SI3). Tau (20 μM) was added to each well together with DTT (1 mM) and a different compound (20 μM), and aggregation was initiated by the addition of heparin (5 μM). CD spectra (190-260 nm) of each well were obtained in 1 h intervals over a 6 h period. From each spectrum was subtracted a baseline spectrum for heparin, DTT and each compound, obtained at the same time interval and ensuring that each cell was matched with the correct compound. Control spectra were also obtained for tau under non-aggregating conditions with only DTT present (number of spectra, n = 10) and for tau with DTT and heparin to induce aggregation (n = 6). Hence, the effect of each compound on aggregation could be compared with the two sets of control spectra at the two extremes.

With large numbers of spectra to process and analyse, it was convenient to apply the multivariate approach of principal component analysis to ascertain which compounds were most effective at stabilising tau in its native un-aggregated structure. Figure 2A shows the principal component (PC) scores plot for the HT-SRCD spectra obtained 3 h after initiating tau aggregation. Each point represents a spectrum of tau in the presence of a compound (black) or of tau under non-aggregating conditions (red outline) or of tau under aggregating conditions (cyan

outline). Within each control group the points cluster closely together, but the two groups are well-separated from each other. This indicates that the variance of the spectra within each group of replicates is much lower than the differences between the spectra of unaggregated and aggregated tau. There is considerable scatter in the compound data, suggesting that the drugs may have a multitude of effects on the structure or aggregation state of tau at this time point. We considered only the points that lie in the same region of the plot as the control data for unaggregated tau, as these points potentially represent the compounds having the largest inhibitory effect. A PC trajectory plot, representing the change in the spectra between 4 h and 6 h (Figure 2B) reveals 2 samples that overlap or lie close to the control data for tau under non-aggregating conditions. These correspond to (+/-)epinephrine hydrochloride (Figure 2C) and (-)-epinephrine bitartrate. All other spectra (represented by arrows outside of the circled region in Figure 2B) indicated partial or full aggregation of tau between 1 h and 6 h, or were not representative of tau in its unaggregated and aggregated structures and possibly consistent with other folding pathways. Follow-up bench-top CD spectra of tau in the presence of epinephrine confirmed that the compound inhibited tau aggregation (Figure 2D).

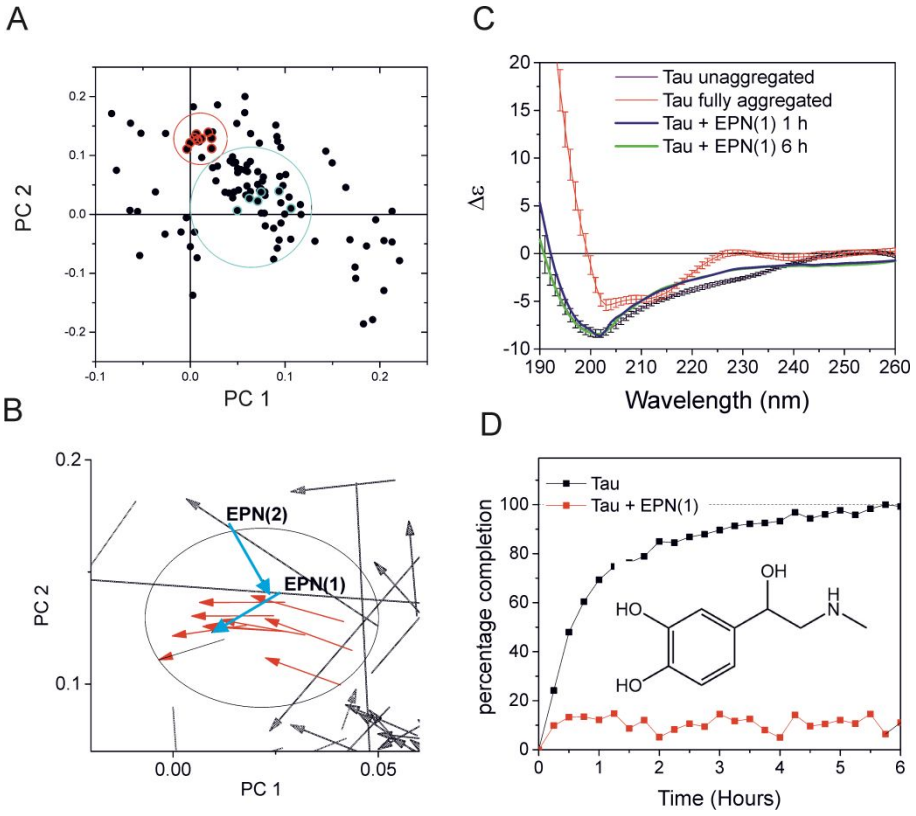

Figure 2. HT-SRCD screening of drug-like compounds for inhibition of tau aggregation. **A**) Principal component score plot representing the variance in the SRCD spectra after incubation of tau with each compound for 6 h. Red outlined circles correspond to the spectra of tau alone under non-aggregating conditions and cyan outlined circles to the spectra of tau alone under aggregating conditions. The red circled area contains data for the compounds having the greatest inhibitory effect and the cyan circled area represent spectra showing partial or full aggregation of tau. **B**) A PC trajectory plot representing the change in the SRCD spectra from 1 h to 6 h. The red arrows represent the spectra of tau under non-aggregating conditions. Cyan arrows within the circled region represent the compounds eliciting the largest inhibitory effect, racemic epinephrine hydrocholride (EPN(1)) and (-)-epinephrine bitartrate (EPN(2)). **C**) Comparison of the HT-SRCD spectra of tau with EPN(1) (blue/green lines) with the spectra of tau under non-aggregating conditions at t = 0 (black lines; n = 10) and of tau in the presence of heparin after 6 h (red lines; n = 6). **D**) Follow-up far-UV CD spectra of heparin-induced tau aggregation obtained on a bench-top instrument alone (black) and in the presence of EPN(1) (red). Aggregation was monitored by measuring Δε at 218 nm.

Identification of salbutamol as a tau aggregation inhibitor

HT-SRCD indicates that epinephrine is superior to all other drugs screened, which cover a wide chemical space, in its ability to inhibit tau aggregation *in vitro*, and is therefore a good starting point from which to identify chemically similar compounds that may have more favourable properties *in vivo*. Epinephrine is one of several catechol-containing molecules that has previously been reported as an Aβ, α-synuclein and tau aggregation inhibitor;[37,38] here we show for the first time that it stabilises the native protein structure. Several other molecules possessing a catechol moiety, including dopamine[38] and norepinephrine,[39] have been shown to modulate Aβ fibril formation. Catechols block the formation of toxic oligomers by tau in a mechanism that may involve oxidation to quinones and subsequent capping of tau cysteine residues,[37] although non-covalent interactions may also play a role. The major challenge in progressing catechol and polyphenolic compounds as AD therapeutics is their low bioavailability: they are poorly absorbed when ingested and are highly susceptible to metabolic transformations (principally oxidation, glucuronidation, methylation and sulfation),[40–42] being substrates for catechol-*O*-methyltransferases.[43,44]

To mitigate this anticipated problem in future *in vivo* evaluations, we searched for chemically-similar marketed drugs for other disease indications, but which may have more favourable bioavailability than epinephrine. The HT-SRCD screen revealed that two metabolites of the dopamine-epinephrine biosynthetic pathway included in the 96-well plate, (±)-vanillylmandelic acid and dihydroxyphenylalanine, did not impede tau aggregation despite their structural relationship with and similarity to epinephrine (Figure 3). Hence, it could not be assumed *a priori* that epinephrine analogues would be effective inhibitors, and further empirical studies were necessary to establish a structure-activity relationship.

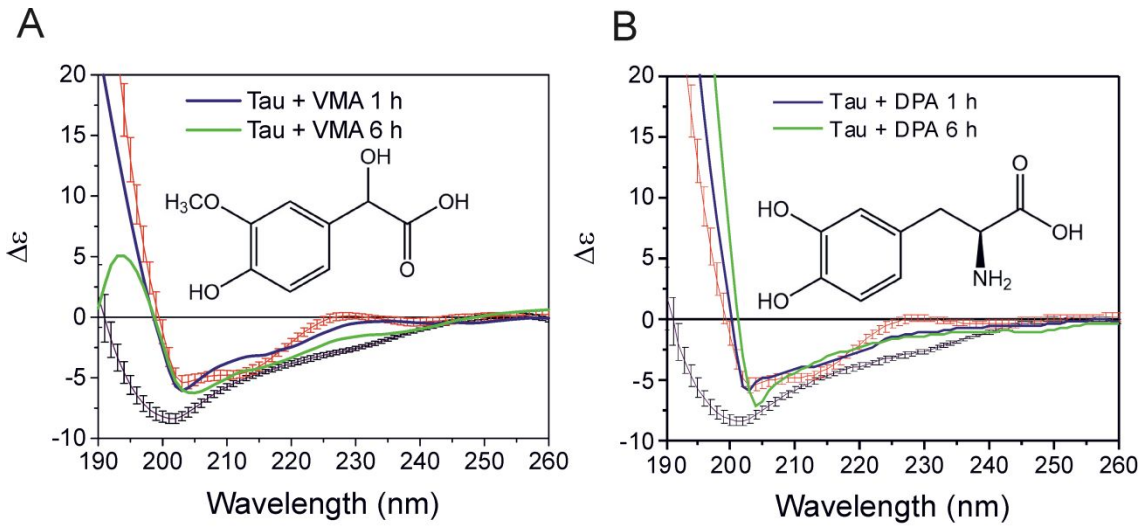

Figure 3. Comparison of the HT-SRCD spectra of non-aggregated tau (black with error bars) and fully aggregated tau (red with error bars) with the spectra of tau (20 μM) in the presence of equimolar (±)-vanillylmandelic acid (VMA) (**A**) or dihydroxyphenylalanine (DPA) (**B**).

After a similarity search, four drug compounds, etamivan, fenoterol, dobutamine and salbutamol, were selected for further screening against tau aggregation (Figure 4). All have chemical features reminiscent of epinephrine, but only dobutamine possesses the metabolically-labile catechol moiety. Fresh tau solutions were incubated with shaking for up to 24 h with heparin in the presence of equimolar concentrations of each compound and aggregation was monitored by far-UV CD, using a bench-top instrument. The spectra of tau with fenoterol and etamivan suggest that neither compound has a significant effect on the aggregation kinetics (Figure 4, A and B) and fenoterol appears to enhance the rate of aggregation. Interference and distortion below 210 nm preclude a rigorous analysis of secondary structure that would confirm that tau follows the normal aggregation pathway. In the presence of dobutamine, the characteristic spectral perturbation and presence of an isodichroic point (at 207 nm) is observed, suggesting a single-phase structural change still occurs in presence of dobutamine and reaches

completion by 5 h (Figure 4A). The half time, $t_{0.5}$, for completion of aggregation is similar to the native tau (Figure 4B), but SSE using the BeStSel algorithm indicates that a negligible change in β–sheet content (2 %) occurs after 24 h, with only a slight decrease of 3.5 % in the unordered content (Figure 4C). Hence, although the kinetics of the tau structural transformation appear to be unaffected by dobutamine, aggregation does not appear to run to the same extent as for tau alone.

After incubation of tau with salbutamol for up to 24 hours, the spectrum remains largely unchanged and there is no isodichroic point of the initial and end spectra (Figure 4A). Hence, the spectra suggest that only minor structural changes occur over this time scale, or that the structural perturbation is more complex than the transition between two species. Interestingly, the β-sheet content reduces in the presence of salbutamol to 25.9 ± 3.6 %, with an increase in the unordered content of 14.7 % (Figure 4C). Comparison of the $t_{0.5}$ (measured from Δε at 218 nm) reveals that salbutamol impedes the conversion from the starting to the end conformation, although this figure is no longer reflective of a single-phase transition (Figure 4B). The CD data suggests that salbutamol impairs tau aggregation and stabilises tau in a structure close to its initial native state. By contrast, dobutamine appears not to have a significant effect on the rate of tau structural modification.

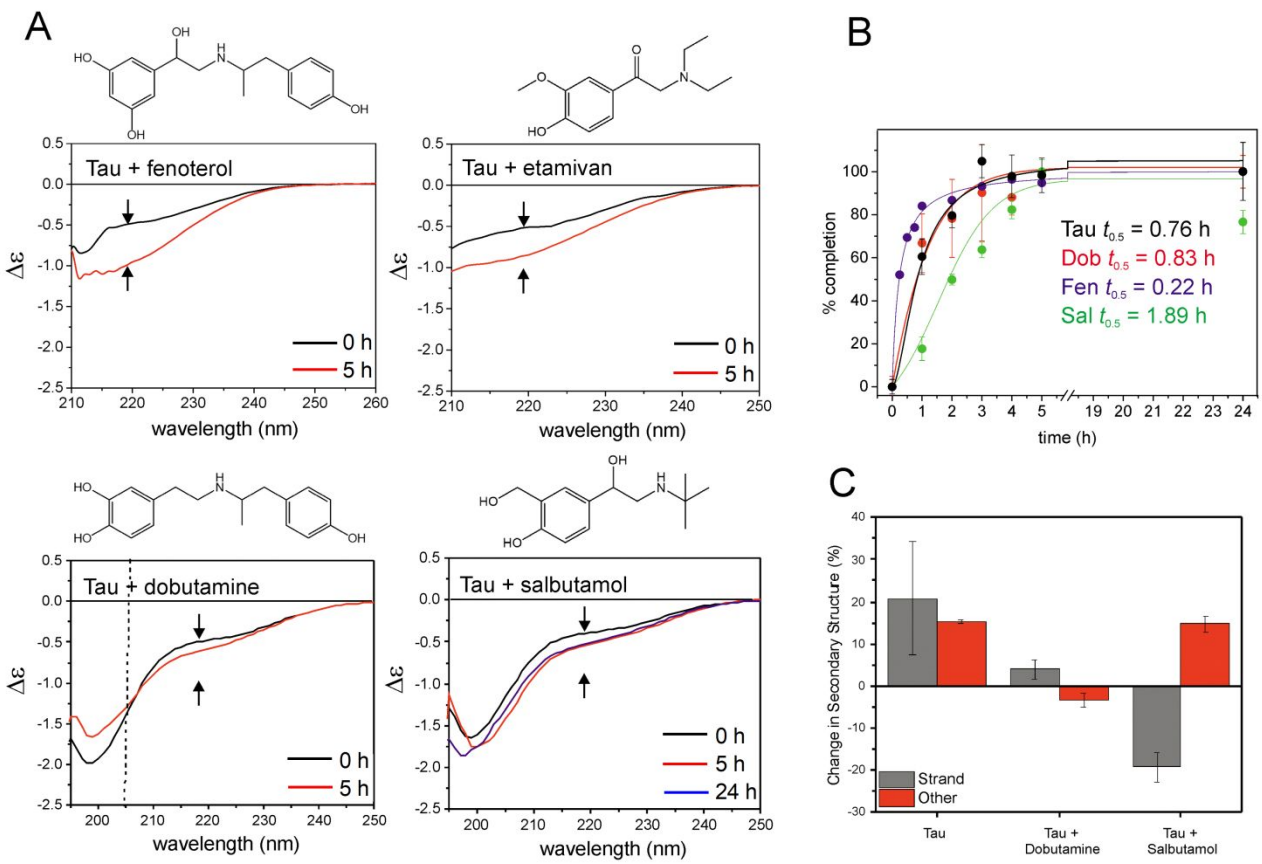

Figure 4. **A)** Far-UV CD spectra of tau (20 μM) after incubation for 0 (black) and 5 h (red) in the presence of equimolar concentrations of four catecholamine-derived β_2-adrenergic receptor agonists. In order to focus the attention to the spectral features of tau, the CD contributions of the bound fenoterol and etamivan appeared below 210 nm are not shown. The double arrows represent the increase in Δε measured at 218 nm (consistent with β-sheet formation) from the spectra of tau alone at 0 and 5 h. For salbutamol, an additional spectrum is shown after 24 h incubation (blue). **B**) Kinetics of tau aggregation in the presence of the four compounds, monitored by the change in Δε at 218 nm. **C**). Percentage change in secondary structure of tau in the presence of dobutamine and salbutamol, estimated by the BeStSel algorithm,[35] following incubation for 5 h.

For fenoterol, an RR and SS racemate, the appearance of CD contributions when freshly added to tau signify a difference in the binding between the two enantiomers with tau. For achiral etamivan the induced CD is the result of the binding to the chiral binding site of tau. In both cases, the non-superimposable spectra to that of tau alone indicate unambiguously binding interactions between these molecules and tau. However, for wavelength greater than 210 nm though these CD contributions are small or negligible, the shape profile of the CD can still be used to discriminate qualitatively significant conformational changes and taken as diagnostic of the aggregation of tau protein.

For both racemate dobutamine and salbutamol, the fact that in the presence of equimolar tau protein, the CD spectra of the freshly made mixtures still resembled those of tau alone (Figure 4A) and did not change significantly with ageing, indicate their inhibitory tau aggregation property. It also indicates that the binding interactions in terms of chirality is similar for the enantiomers cancelling out, leaving mainly the CD contributions from tau.

Among the 88 LOPAC^{1280} samples screened with tau, the CD of dobutamine and salbutamol were the ones with the highest similarity to that of the monomeric form of tau with minimum changes as a function of time revealing their inhibitory property against tau's aggregation.

Tau aggregation kinetics monitored by Thioflavin T

Tau aggregation *in vitro* into insoluble filaments coincides with increased β-sheet structure and reactivity to the amyloid specific dye ThT, which can be used to follow the kinetics of tau self-assembly into amyloid.[33,45,46] Here, ThT was used to study the kinetics of tau aggregation in the presence of fenoterol, dobutamine and salbutamol, respectively. Figure 5A indicates that tau self-assembly coincides with a time-dependent sigmoidal increase in ThT fluorescence intensity

representing overlapping prenucleation, nucleation, filament elongation and maturation/termination steps.[47] Fenoterol at 10 μM had no significant effect on the tau aggregation rate or yield of filaments (as represented by the end-point fluorescence) and at 20 μM the drug increased the rate of aggregation, as also observed in the CD analysis (Figure 4B). Addition of dobutamine or salbutamol reduced the end-point fluorescence intensity, with salbutamol being more effective than dobutamine at lower (1.25 μM and 5 μM) concentrations (Figure 5 B and C). The normalised ThT profile for tau alone (Figure 5 D and E) agrees well with a curve calculated for specific values of the rate constants for primary nucleation (k_n), fibril elongation (k_+) and fragmentation (k_-), and secondary nucleation (k_2) as well as the reaction order for the primary (n_c) and secondary (n_2) processes.[48] The data for tau treated with dobutamine and salbutamol reveal that both compounds increase $t_{0.5}$ for completion of aggregation (Figure 5, D and E). Good fits of calculated curves to the ThT profiles are achieved by decreasing only the primary nucleation rate constant k_n, from 2 x 10^{-5} M^{-1} s^{-1} to 9 x 10^{-6} M^{-1} in the presence of equimolar dobutamine and to 1 x 10^{-5} M^{-1} s^{-1} for salbutamol. It should be noted, however, that without global curve fitting to ThT data obtained at different tau concentrations there is uncertainty in the values of these constants. With this caveat, the fitting suggests that the compounds interact with pre-nucleation species of tau formed during the lag phase, reducing their ability to form a critical nucleus.

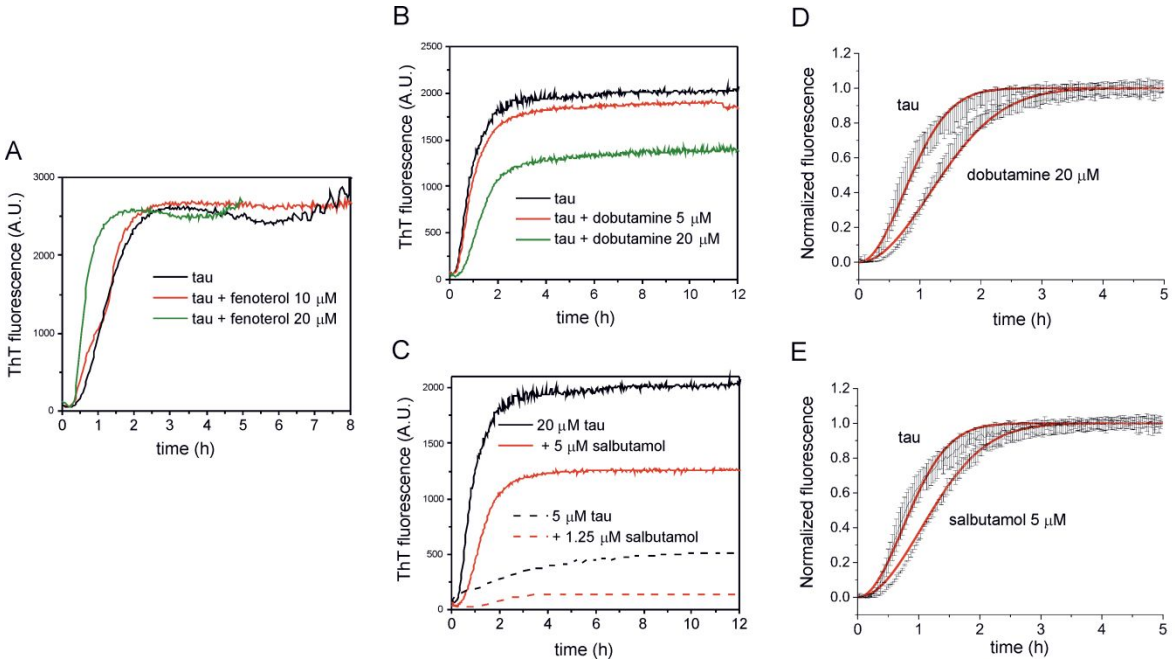

Figure 5. Effects of catecholamine-derived β_2-adrenergic receptor agonists on tau aggregation monitored by time-resolved ThT fluorescence. **A-C**) Aggregation kinetics of 20 μM tau alone (solid black line) or in the presence of different concentrations of fenoterol (**A**), dobutamine (**B**), and salbutamol (**C**). The experiment of tau in the presence of salbutamol was also repeated at lower concentrations of tau whilst maintaining the molar ratio. Each line represents the mean of measurements in triplicate over 12 h. **D**) Normalised ThT fluorescence of tau alone and with 20 μM dobutamine. **E**) Normalised ThT fluorescence of tau alone and with 5 μM salbutamol. Error bars in (**D**) and (**E**) represent the standard deviations from triplicate measurements. Red lines were calculated from the equations of Cohen et al.[48] For tau alone, the line of best fit (red) corresponds to: $k_n = 2 \times 10^{-5}$ M^{-1} s^{-1}, $k_+ = 6 \times 10^6$ M^{-1} s^{-1}, $k_- = 3 \times 10^{-2}$ $M^{-1}s^{-1}$, $k_2 = 1 \times 10^{-4}$ M^{-1} s^{-1}, $n_c = 2$, $n_2 = 2$. For tau with dobutamine the line of best fit was obtained by increasing k_n to 9×10^{-6} M^{-1} s^{-1} and for tau with salbutamol increasing k_n to 1×10^{-5} M^{-1} s^{-1}. All other parameters were kept constant.

It is not surprising that dobutamine, carrying a catechol moiety, inhibits tau aggregation because of its similarity to other inhibitory catecholamines,[37] but the discovery that salbutamol has a larger effect, and at lower concentrations, is a more interesting prospect warranting further

evaluation. Salbutamol, a β_2-adrenergic agonist and widely-used asthma therapy with a good safety profile, does not bear a catechol moiety or a primary amine group, which extends its half-life *in vivo* and facilitates rapid permeation through the blood brain barrier to about 5 % of the plasma concentration.[49] Dobutamine, on the other hand, is a short-lived drug administered intravenously for treatment of acute heart failure and cardiogenic shock, and would be of little value as an AD therapy. We therefore restricted further analysis to salbutamol only.

Congo red confirms that salbutamol inhibits tau aggregation *in vitro.*

Phenolic compounds have been shown to produce a false positive effect when screened for inhibition of amyloid self-assembly using ThT fluorescence.[30,50] This is because some polyphenols absorb in the same region of the visible spectrum as ThT (not an issue with salbutamol) but also because the compounds may compete with ThT for the amyloid cross-β binding sites. We applied an alternative method, which exploits the enhancement of Congo red (CR) absorbance upon binding to amyloid.[30] After tau is incubated in the presence of CR for 6 h, by which time aggregation is expected to reach completion, the CR absorbance intensity increases with λ_{max} shifted from 490 nm to 500 nm and the appearance of a shoulder at about 540 nm (Figure 6A). The absorption spectrum of CR alone remains constant over this period and, as expected, tau alone contributes little in this region of the spectrum (Figure 6, B and C). When tau and CR are incubated with salbutamol for 6 h, the changes in the spectrum that accompany tau aggregation are not observed (Figure 6D). Instead, only a small local increase in absorbance is seen around 540 nm with a slight decrease in absorbance intensity at λ_{max}. Hence the CR

measurements are consistent with those of ThT indicating that salbutamol inhibits the normal aggregation pathway of tau over the 6 h period.

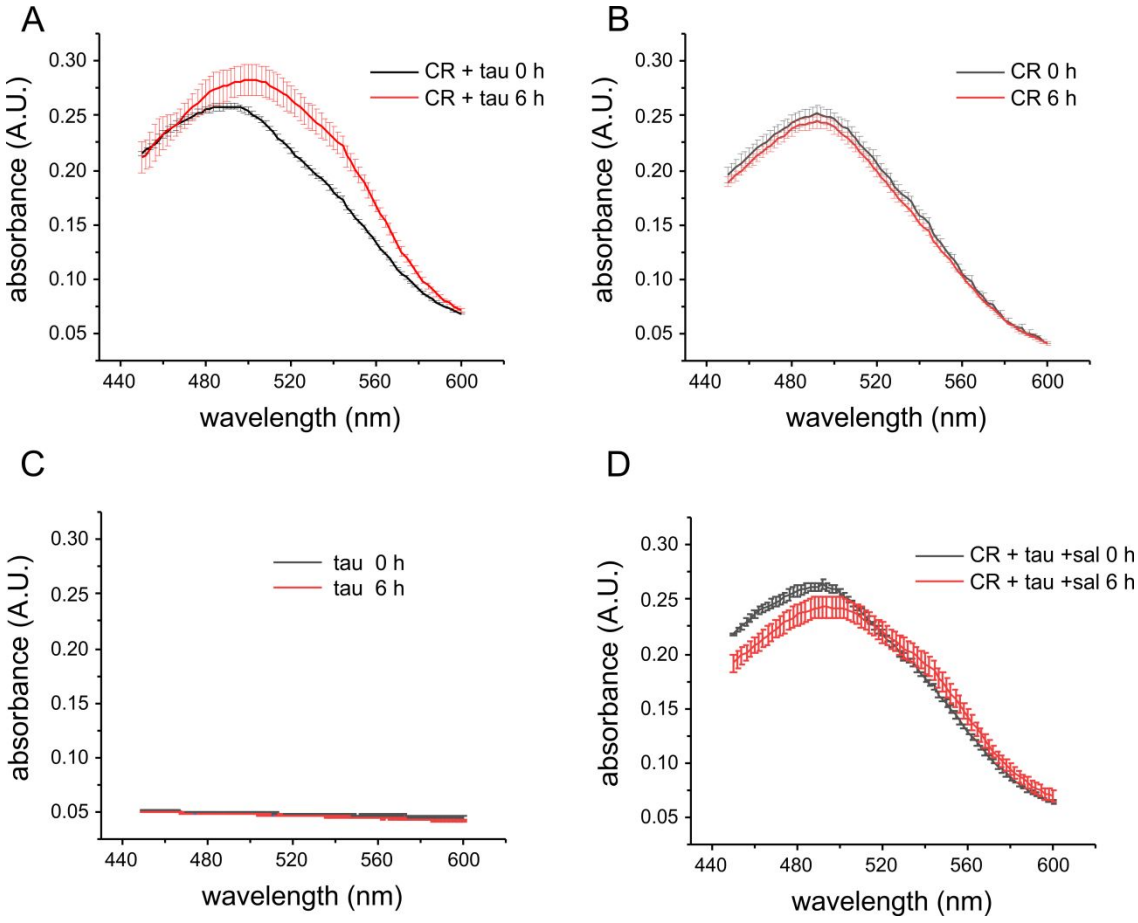

Figure 6. Congo red absorption confirms that salbutamol reduces tau fibril yield. **A)** Tau aggregation monitored by CR absorbance in the visible region (440 – 600 nm) is accompanied by an enhancement in the absorbance band after 6 h and a red shift of λ_{max}. The spectra of CR alone (**B**), tau alone (**C**), or salbutamol and CR (data not shown) show no change over this time period. **D**) In the presence of salbutamol and tau, the absorbance of CR decreases slightly at λ_{max} and increases slightly at around 540 nm. Means and standard errors are shown for triplicate measurements.

Salbutamol binds to the native tau structure

Kinetic analysis of the ThT curves (Figure 5) indicates that dobutamine and salbutamol decrease the nucleation rate constant for tau aggregation, which suggests that the drugs interact with tau monomers or other pre-nucleation species.

To examine this possibility we observed the far-UV and near-UV CD spectra of monomeric, pre-filamentous tau alone and in the presence of salbutamol. Tau aggregation does not occur for at least 6 h by omitting heparin and DTT from the protein solution according to ThT assay and the protein retains its initial conformation as confirmed by the far-UV CD spectrum (data not presented). Tau is similarly stable in the presence of equimolar salbutamol under these conditions (Figure 7A). The aromatic region of the near-UV CD spectra was then observed to detect an interaction between salbutamol and pre-filamentous tau. In the absence of salbutamol the negative CD from 260-300 nm is attributed to the 2 tyrosine and 2 phenylalanine residues of tau (Figure 7B). The negative CD in this region is enhanced in the presence of equimolar salbutamol (Figure 7B and C). Salbutamol is synthesized as a racemate in which the *R*-enantiomer has a 150-fold high affinity for β-adrenoreceptors than the *S*-enantiomer,[51] the latter has for a long time been considered pharmacologically inactive and linked to adverse toxicity.[52] The racemate alone does not show a CD spectrum whereas the R-enantiomer (called levalbuterol) does (Figure 7D), hence the CD enhancement in the presence of tau must arise either from a perturbation of the racemic mixture (e.g., by the two enantiomers interacting differently with tau) or from a perturbation of the protein aromatic residues, or both. Nevertheless, the CD spectral changes in the near-UV range is diagnostic of a binding interaction between one or both salbutamol enantiomers with tau.

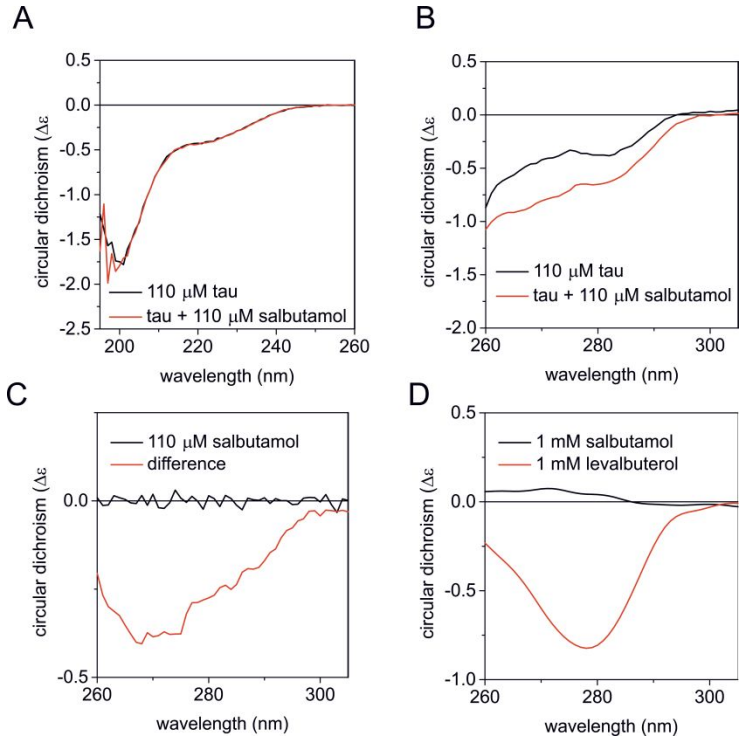

Figure 7. Interaction of salbutamol with pre-filamentous tau. **A**) Far-UV CD spectra of tau (110 μM) in the absence of heparin and DTT. **B**) Near-UV CD spectra of tau (110 μM) in the absence of heparin and DTT before (black line) and after (red line) the addition of 110 μM salbutamol. **C**) Near UV CD spectrum of the salbutamol racemate (110 μM) alone (black line) and a difference spectrum (red) obtained by subtracting the spectrum of tau with salbutamol from the spectrum of tau alone. **D**) Near UV CD spectrum of 1 mM salbutamol racemate (black) and levalbuterol (red). The spectrum shown is the average of 3 scans.

Salbutamol influences the fibril morphology of tau

In the presence of heparin, tau aggregates into insoluble aggregates after 24 h and visualisation by negative staining transmission electron microscopy (TEM) reveals a loose mesh of interwoven filaments with typical amyloid morphology, consisting of networks of long unbranched fibres

from 500 nm to 1 μm (Figure 8A). Treatment of tau with salbutamol results in the deposition of fibrillar structures with different morphologies to the untreated tau. In the presence of salbutamol the filament density is drastically reduced, with the filaments sparsely distributed. However, these remaining filaments are considerably longer in length than the untreated tau fibrils, and possess regular repeating twists, causing a coiled effect (Figure 8B). This could possibly suggest a preference for the paired helical filament structures commonly observed in tau deposits. The TEM images concur with ThT and CD and indicate that salbutamol interferes with fibril formation of tau.

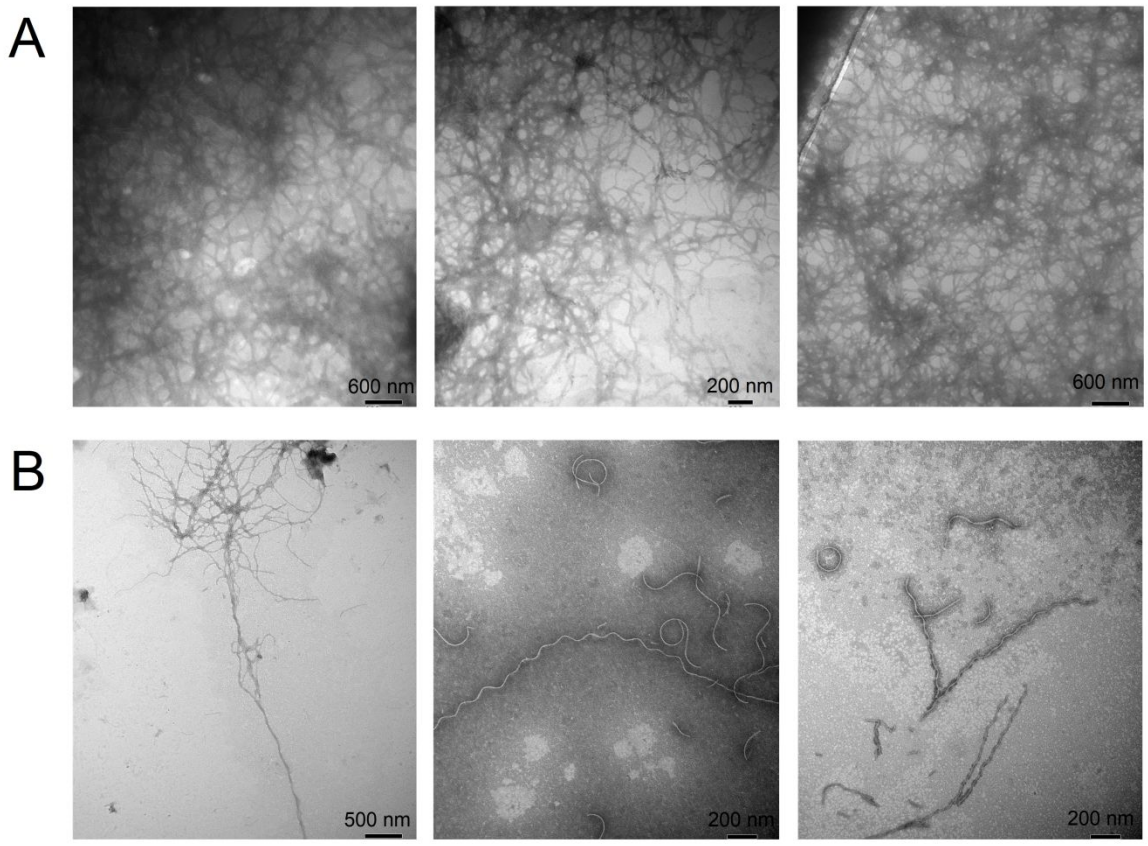

Figure 8. Negatively stained TEM images of tau (20 μM) aggregates formed in the presence of heparin (5 μM) after 24 hours incubation at 37 °C (**A**) and with the addition of 20 μM salbutamol (**B**). Three different regions of the TEM grids are shown for each sample group.

Molecular docking of salbutamol to tau fibrils

Currently, no structure of monomeric tau, dissociated from microtubules, is available in the protein databank (PDB). This restricts the docking of compounds to the pre-nucleation species where, given the data presented here, it appears salbutamol interferes with tau self-assembly. Instead, the compounds investigated above, in addition to the amyloid diagnostic dye thioflavin T and epigallocathin-3-gallate (EGCG), a known inhibitor of tau aggregation *in vitro*, were docked to a model of heparin induced tau amyloid (PDB: 6QJH)[53] using ICM Pro (Molsoft)[54–57] to compare the binding energies.

ICM Pro identified 8 binding pockets in this model of tau, (Figure 9A) of which only the largest pocket by volume (Pocket 1) was predicted to be drugable with a Merck's score of 1.19 exceeding the 0.5 cut off, with all other pockets having values below this (SI Table 1). The majority of the compounds screened interact with this largest pocket, apart from thioflavin T (Pocket 2) and fenoterol (Pocket 3). This suggests the reduction in ThT fluorescence by tau in the presence of salbutamol, dobutamine and epinephrine, and therefore their apparent inhibition of amyloid formation, is unlikely to be a type I (false positive) error caused by competitive binding interference with the ThT dye.

EGCG is included in the list of compounds docked due to observations elsewhere of its inhibitory effect on amyloid proteins including tau,[58] although its ability to interfere with heparin induced tau amyloidosis is limited, and results only in a changed morphology.[59] Here, the overall binding energy for EGCG (ICM grid docking energy = 6.8) to the heparin induced tau model is considerably lower than many of the other compounds, including salbutamol (ICM grid docking energy = -18.77) (SI Table 2). Despite this, both EGCG and salbutamol bind in the drugable pocket, and both are stabilised by 2 hydrogen bonds. EGCG forms two hydrogen bonds with tau

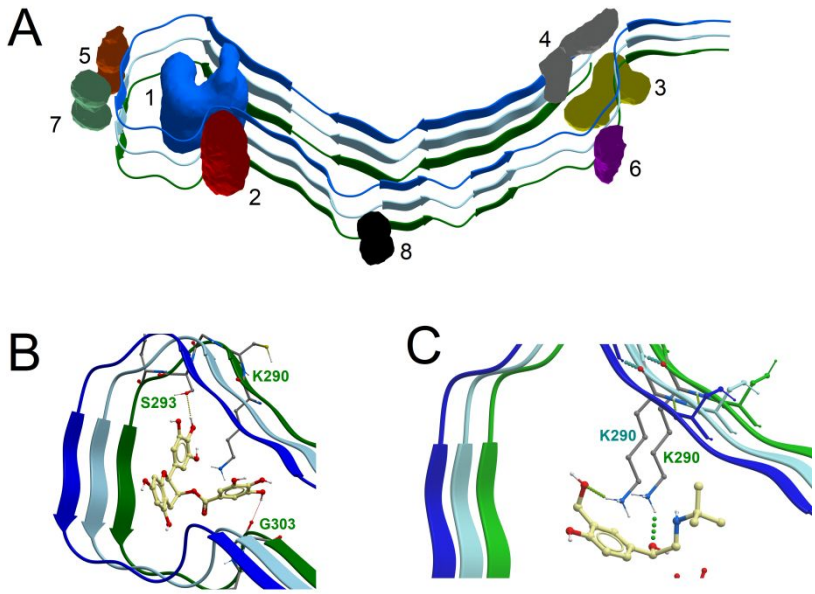

Figure 9. ICM PRO pocket finder (**A**) highlighting the 8 possible binding regions, and the binding location and orientation of EGCG (**B**) and salbutamol (**C**) within binding pocket 1, with hydrogen bonds depicted with spherical dotted lines.

between the phenolic hydroxy group and the hydroxy side chain of serine (293), and between a hydroxy group on the gallate component of EGCG and the carbonyl backbone of glycine (303), with both bonds forming within the same tau molecule (Figure 9B). These residues are on opposite sides of the horseshoe fold surrounding Pocket 1, and this cross-liking could offer stabilisation of the tertiary fold. Salbutamol also forms 2 hydrogen bonds between the phenolic hydroxymethyl and the amine side chain of lysine (290) on one tau molecule, and between the hydroxy group and the amine side chain of lysine (290) on a second molecule. The interaction of salbutamol with 2 tau molecules vertically along the fibril axis, rather than within the single molecule, could explain how salbutamol interferes with heparin induced tau amyloidosis. GAGs such as heparin commonly form an initial interaction with amyloid species and acts as a scaffold

structure, supporting amyloid formation.[60–63] The binding of salbutamol across multiple tau monomers may disrupt this interaction, thereby reducing the formation of the prenucleation species, and subsequently modulating tau elongation (Figure 9C).

Conclusion

Developing new drug entities is costly and slow, with a high attrition rate, but with the pressing economic burden of AD there is a strong motivation to expedite the R & D process. One attractive approach is to repurpose existing drugs clinically approved for other indications. This has been explored for indomethacin, a nonsteroidal anti-inflammatory drug which has shown additional activity against AD in both cellular and mouse models by reducing the processing of the aggregation-prone Aβ.[64] Carvedilol, a non-specific adrenergic antagonist, interferes with the amyloid self-assembly mechanism directly and prevents the formation of fibrils.[65] Here we show that two established β-adrenergic agonists, salbutamol and dobutamine modulate tau filament formation by the AD protein tau *in vitro*. Many successful small compound inhibitors of amyloid do so by one of three mechanisms: (i) stabilisation of the native structure, (ii) directing assembly towards a non-amyloid structure or a non-toxic oligomeric species, or (iii) interfering with the β-sheet formation.[66,67]

High throughput CD investigations into the structural transition tau undergoes during self-assembly is a novel way to screen libraries of compounds without the competing effects of using amyloid diagnostic dyes, such as Thioflavin T or Congo red. Using this technique, we confirmed that the known amyloid inhibitor epinephrine stabilised the native structure of tau, limiting its transition into β-sheet rich species, although several of its metabolic intermediates did not,

emphasising the necessity for a structural HTP screening technique. Searches for structurally similar compounds identified 4 potential candidates already marketed for alternative therapeutic uses: etamivan, fenoterol, dobutamine and salbutamol. Further investigations suggested neither etamivan nor fenoterol had any significant effect on the kinetics of tau self-assembly.

Dobutamine is a β_1-adrenergic receptor agonist possessing both polyphenolic and catechol moieties. Its effects are short-lived due to the unmodified catechol moiety making it labile to methyl-o-transferase, and it is administered intravenously for rapid treatment of cardiogenic shock and severe heart failure. Here we find that, as reported for other catechols, dobutamine interferes with amyloid fibril formation by tau. Salbutamol, a selective β_2-adrenergic receptor agonist, is a catecholamine derivative with a modified methylhydroxy catechol group, preventing its degradation by catechol-*O*-methyltransferases.[68] Here, observations using four independent techniques indicate that salbutamol markedly impairs tau self-assembly. Salbutamol reduces the rate of tau aggregation, apparently by stabilising the native unaggregated structure, and markedly reducing the amount of fibril deposition into twisted strands that closely resemble paired helical filaments.

These findings indicate that the catechol moiety or primary amine, one or both functionalities being features of many endogenous or plant-derived amyloid inhibitors, are not essential for inhibition of tau's aggregation. This is an important finding in an AD context, as removal of these functionalities confer greater bioavailability and pharmacokinetics on salbutamol compared to catechol(amines)s. Under normal physiological conditions, catecholamines, including epinephrine, are metabolised by monoamine oxidase (MAO) into the non-toxic 3-4-dihydroxymandelic acid and hydrogen peroxide. However, due to the impaired antioxidant defence system and increase in reactive oxygen species in neurodegenerative

diseases, alternative pathways are triggered resulting in the production of *o*-semiquinone, *o*-quinone, and subsequently nitronorepinephrine species.[69] The latter impedes catechol-*o*-methyl transferase activity and the neuronal update of norepinephrine, further promoting neurodegeneration.[70] In the absence of the catechol moiety, salbutamol does not undergo the same catalysed oxidation to *o*-semiquinone or *o*-quinone species. β_2-adrenoceptor agonists, such as salbutamol, are primarily metabolised in the airways and gastrointestinal tract by stereoselective sulfate conjugation, leading to an accumulation of the inactive *S*-enantiomer.[71] However, oxidation by inflammatory peroxidases, such as myeloperoxidase (MPO) and to a lesser extent lactoperoxidase (LPO), is also viable, forming free radical species and structurally modified derivatives, including *o*,*o*'-disalbutamol.[72] Whilst expression of MPO is often increased in inflamed brain regions associated with AD and parkinsons,[73,74] this is not the primary metabolic pathway for βAR agonists, and salbutamol itself has been shown to possess antioxidant activity against ROS and decrease MPO and LPO oxidation activity.[75]

The challenges of targeting tau and Aβ aggregation in the brain are formidable and to justify further evaluation of salbutamol, and/or related compounds, in animal models of AD one must consider their bioavailability, specificity and pharmacokinetics. Salbutamol does enter the brain in low concentrations when administered at high doses, but dobutamine has poor penetration across the blood-brain barrier,[51,76] although it is worth noting that isoprenaline, another catecholamine with predicted poor brain penetration, reduces the level of detergent insoluble tau in mouse brains.[64] Salbutamol has a half-life of 2.7-5 hours and dobutamine of 2 minutes.[51] Clearly, the primary role of these compounds in activating β_1 and β_2-adrenergic receptors must also be considered. β_2-adrenoreceptor stimulation has been shown to promote the cleavage and release of the amyloidogenic Aβ40/42 peptide via upregulation of the γ-secretase

enzyme,[77] which could have negative consequences for the onset of AD. Conversely, β_2-adrenoceptor activation enhances neurogenesis and ameliorates memory deficits in the APP/PS1 mouse model of AD.[78] Salbutamol is administered as a racemate, but as the R-enantiomer of salbutamol has greater selectivity for β_2-adrenoreceptor than does the S-enantiomer, one could potentially disentangle the effects of receptor stimulation from direct action on tau.

In summary, we have demonstrated *in vitro* ability of βAR agonists to inhibit tau amyloidosis, thus providing the basis for further *in vitro*, and eventually a full *in vivo* evaluation of β-adrenergic receptor agonists as potential therapeutics for AD. Future work would continue to characterise these two compounds for their enantioselective ability to modulate Aβ amyloidosis, in addition to other available βAR agonists that possess the desired pharmacokinetics and ability to permeate the blood brain barrier. Successful drug candidates can then be evaluated in a suitable mouse model, such as the 3xTG, which develops both Aβ and tau amyloid pathologies and would therefore be an ideal model to study the potential dual interference of AD associated amyloidosis by βAR agonists.

3. Methods and Materials

Tau expression

The tau construct used in this work comprises residues 255-441 of human tau from cDNA clone htau46.[31] This isoform consists of the 4 microtubule binding (MTB) repeat units (tau 4R), but with the aggregation impeding N terminus removed, leaving the 2nd and 3rd MTB with the highly amyloidogenic sequences VQIINK and VQIVYK, respectively.[79,80] The protein was expressed and purified as previously described[31].

Effect of dobutamine and salbutamol on the aggregation kinetics of tau

The formation of amyloid was measured with the amyloid specific dye Thioflavin T (ThT). Tau with heparin (20 and 5 μM respectively), was incubated in Tris (30 mM), DTT (1 mM) at pH 7.5 with Thioflavin T (20 μM), alone or in the presence of dobutamine or salbutamol (5-20μM) at 37 °C. Fluorescence measurements, with excitation at 450 nm and emission at 482 nm, were taken from triplicate samples on a Molecular Devices Flexstation 3 Microplate Reader (Molecular Devices), every 2 minutes for 50 hours, with agitation for 10 seconds prior to each read. Normalised ThT data was fitted using the equations detailed in Cohen *et al*.[48] and amending the rate constant k_n until convergence was achieved using the graphical software Origin Pro 2019.

Tau (20 μM) with heparin (5μM), was incubated in Tris (30 mM), DTT (1 mM) at pH 7.5 alone or in the presence of salbutamol (20 μM) at 37 °C for 6 hours. Congo red (20 μM) was added and absorbance spectra acquired on a Flexstation 3 multi-well plate reader between 440-600 nm.

Circular Dichroism.

Tau with heparin (20 and 5 μM, respectively) was incubated in Tris (30 mM), DTT (1 mM) at pH 7.5, alone or in the presence of dobutamine or salbutamol (20 μM) at 37 °C with agitation.

Spectra were acquired hourly during the first 5 hours, followed by acquisition of a final spectra after 24 hours. Spectra were acquired on a Chirascan Plus CD spectrometer between 180 and 260 nm with a band width of 1 nm, using a path-length of 0.2 mm. Background signals of buffer, heparin and the relevant compound were subtracted from the spectra of tau with potential aggregation inhibitors. The content of secondary structure elements in terms of percentage of α-helix, β-strand, turn and unordered conformations was estimated from CD spectra in the 190-260 nm region using BeStSel algorithm.[35]

Far UV spectra of tau alone (110 μM) or in the presence of salbutamol (110 μM) were acquired between 250-350 nm on a Chirascan Plus CD spectrometer with a path-length of 0.2 mm, at Diamond Light Source B23. Subtracting the spectrum of tau alone from the tau with salbutamol spectrum produced differential spectra. Spectra of levalbuterol (1 mM) were later acquired on the same instrument at Lancaster University using a path-length of 2 mm for comparison.

High Throughput Circular Dichroism (HTCD)

Tau with heparin (20 and 5 μM, respectively) was incubated in Tris (30 mM), DTT (1 mM) at pH 7.5, alone or in the presence of compounds from a LOPAC compound library at 37 °C. Samples were prepared in batches of 12 and 15 μL was loaded into a custom-designed 96 plate of fused silica (Suprasil quartz), 1 row at a time using B23 beamline equipped with vertical chamber.[36] Spectra were acquired for each row between 190 and 260 nm with a bandwidth of 1 nm and a pathlength of 0.02 cm, before the next 12 samples were prepared and the process repeated. After completion of all 8 rows, spectra of the entire plate were collected hourly for 6 hours. HTCD spectra from the plates containing the LOPAC library compounds in aggregation buffer were subtracted from the HTCD spectra of incubated tau with heparin and the corresponding LOPAC library compounds (Supporting Information Table SI3).

Transmission Electron Microscopy

Tau with heparin (20 and 5 μM, respectively) was incubated in Tris (30 mM), DTT (1 mM) at pH 7.5, alone, or in the presence of dobutamine or salbutamol (20 μM) at 37 °C for 24 hours with agitation. A 10 μL suspension was spotted onto carbon coated formar grids (Agar Scientific, UK). After 5 minutes the excess liquid was removed via blotting. For negative staining, 10 μL of 2 % phosphotungstic acid was spotted onto the loaded grids, and left for 3 minutes before blotting the excess. Grids were viewed on a Jeol JEM-1010 electron microscope and images captured at 80 KV with an AMT Nanosprint500 digital camera (Deben, UK) were representative of the entire grid.

ICM Docking

All molecular docking models were based on the cryo-EM structure of heparin induced 2N4R filaments (PDB 6QJH)[53] in order to replicate the conditions used throughout this study, and all simulations were completed on Molsoft ICM Pro 3.9-1a software. The PDB 6QJH file was converted to the ICM file, with tightly bound water molecules remaining, and hydrogen, histidine, proline, glutamate, glycine and cysteine residues were all optimised. Binding pockets were identified using the ICM Pro pocket finder algorithm with a tolerance of 3 and ordered by their volume in table S1. The ICM file of 6QJH was prepared for docking, ensuring the box covered the entire protein surface and the initial ligand position left in its automatically selected starting location. Docking was initiated by creating a chemical table of the individual compound from the ChEMBL database, and docking to the ICM file of 6QJH with a thoroughness of 10 and 3 conformations, with racemic species sampled.

Abbreviations

Amyloid beta (Aβ), Amyloid beta 1-40 (Aβ40), Alzheimer's Disease (AD), Amyloid Precursor Protein (APP), β-Adrenergic Receptor (β-AR), Beta Structure Selection (BeStSel), Circular Dichroism (CD), Dithiothreitol (DTT), Dynamic Light Scattering (DLS), Epigallocatechin-3-gallate (EGCG), High-throughput (HT), Lactoperoxidase (LPO), Methionine Capped Amyloid Beta 1-40 (MAβ40), Microtubule Associated Protein Tau (MAPT), Microtubule Binding (MTB), Monoamine oxidase (MAO), Myeloperoxidase (MPO), Neurofibrillar Tangles (NFT), Secondary structure estimation (SSE), synchrotron radiation (SR), Thioflavin T (ThT).

Author Information:

Corresponding Author: David J Townsend[†] (Email:d.townsend1@lancaster.ac.uk)

Authors: Barbora Mala[†], Eleri Hughes[†], Rohanah Hussain[‡], Giuliano Siligardi[‡], Nigel J. Fullwood[§], & David A. Middleton[†].

[†] Department of Chemistry, Lancaster University, Lancaster, LA1 4YB, United Kingdom.

[‡] Diamond Light Source Ltd., Diamond House, Harwell Science & Innovation Campus, Didcot, OX11 ODE, Oxen, United Kingdom

[§] Biomedical and Life Sciences, Lancaster University, Lancaster, LA1 4YG, United Kingdom

Author Contributions

D.M. and D.T devised the project and wrote the manuscript. Experiments were designed and conducted by D.T., B.M., G.S., R.H., and N.J.F. All authors contributed and reviewed the results and approved the final version of the manuscript. The authors declare no conflict of interest.

Acknowledgements: We thank Prof. David Allsop[§] and Anthony Aggidis[§] for providing the tau plasmid construct through their ongoing collaboration with Prof. Masato Hasegawa, and Dowager Countess Eleanor Peel Trust for the TEM digital camera used in this project.

Supporting Information:

Table SI1. Output from the ICM Pro (Molsoft) pocket finder algorithm for the heparin induced 2N4R tau filament (PDB 6QJH).

Table SI2. ICM Pro (Molsoft) predicted binding energies for compounds docked to the heparin induced 2N4R tau filament (PDB 6QJH).

Table SI3. List of compounds from the LOPAC^{1280} series used in the high-throughput SRCD screening.

References

(1) Prince, M.; Comas-Herrera, A.; Knapp, M.; Guerchet, M.; Karagiannidou, M. World Alzheimer Report 2016: Improving Healthcare for People Living with Dementia. https://www.alz.co.uk/research/WorldAlzheimerReport2016.pdf (accessed Apr 21, 2020).

(2) Prince, M.; Wimo, A.; Guerchet, M.; Gemma-Claire, A.; Wu, Y.; Prina, M. World Alzheimer Report 2015: The Global Impact of Dementia - An analysis of prevalence, incidence, cost and trends.https://www.alz.co.uk/research/WorldAlzheimerReport2015.pdf (accessed Apr 21, 2020).

(3) Patterson, C. World Alzheimer Report 2018: The state of the art of dementia research. https://www.alz.co.uk/research/WorldAlzheimerReport2018.pdf (accessed Apr 21, 2020).

(4) Lane, C. A.; Hardy, J.; Schott, J. . Alzheimer's Disease. *Eur. J. Neurol.* **2018**, *25*, 59–70.

https://doi.org/10.1111/ene.13439.

(5) Graham, W. V.; Bonito-Oliva, A.; Sakmar, T. P. Update on Alzheimer's Disease Therapy and Prevention Strategies. *Annu. Rev. Med.* **2017**, *68* (1), 413–430. https://doi.org/10.1146/annurev-med-042915-103753.

(6) Nisbet, R. M.; Carlos, J.; Ittner, L. M.; Götz, J. Tau Aggregation and Its Interplay with Amyloid-β. *Acta Neuropathol.* **2015**, *129*, 207–220. https://doi.org/10.1007/s00401-014-1371-2.

(7) Kumar, A.; Singh, A. A Review on Alzheimer ' s Disease Pathophysiology and Its Management : An Update. *Pharmacol. Reports* **2015**, *67* (2), 195–203. https://doi.org/10.1016/j.pharep.2014.09.004.

(8) Kurz, A.; Perneczky, R. Novel Insights for the Treatment of Alzheimers Disease. *Prog. Neuropsychopharmacol. Biol. Psychiatry* **2011**, *35* (2), 373–379. https://doi.org/10.1016/j.pnpbp.2010.07.018.

(9) Monge-bonilla, A. S. I. A. C. Molecular Pathogenesis of Alzheimer ' s Disease : An Update. *Ann. Neurosci.* **2017**, *24*, 46–54. https://doi.org/10.1159/000464422.

(10) Felice, F. G. De; Wu, D.; Lambert, M. P.; Fernandez, S. J.; Velasco, P. T.; Lacor, P. N.; Bigio, E. H.; Jerecic, J.; Acton, P. J.; Shughrue, P. J.; Chen-dodson, E.; Kinney, G. G.; Klein, W. L. Alzheimer's Disease-Type Neuronal Tau Hyperphosphorylation Induced by Aβ Oligomers. *Neurobiol. Aging* **2008**, *29* (9), 1334–1347. https://doi.org/10.1016/j.neurobiolaging.2007.02.029.

(11) Lee, V. M. .; Goedert, M.; Trojanowski, J. Neurodegenerative Taupathies. *Annu Rev Neurosci* **2001**, *24* (1), 121–159.

(12) Holmes, C.; Boche, D.; Wilkinson, D.; Yadegarfar, G.; Hopkins, V.; Bayer, A.; Jones, R. W.; Bullock, R.; Love, S.; Neal, J. W.; Zotova, E.; Nicoll, J. A. Long-Term Effects of Aβ42 Immunisation in Alzheimer's Disease: Follow-up of a Randomised, Placebo-Controlled Phase I Trial. *Lancet* **2008**, *372* (9634), 216–223. https://doi.org/10.1016/S0140-6736(08)61075-2.

(13) Rapoport, M.; Dawson, H. N.; Binder, L. I.; Vitek, M. P.; Ferreira, A. Tau Is Essential to β-Amyloid-Induced Neurotoxicity. *Proc. Natl. Acad. Sci. U. S. A.* **2002**, *99* (9), 6364–6369. https://doi.org/10.1073/pnas.092136199.

(14) Roberson, E. .; Scearce-Levie, K.; Palop, J. .; Yan, F.; Cheng, I. .; Wu, T.; Gerstein, H.; Yu, G.; Mucke, L. Reducing Endogenous Tau Ameliorates Amyloid B–Induced Deficits in an Alzheimer's Disease Mouse Model Erik. *Science (80-.).* **2007**, *316* (May), 750–754.

(15) Arriagada, P. V.; Growdon, J. H.; Hedley-Whyte, E. T.; Hyman, B. T. Neurofibrillary Tangles but Not Senile Plaques Parallel Duration and Severity of Alzheimer's Disease. *Neurology* **1992**, *42* (3), 631–639. https://doi.org/10.1212/wnl.42.3.631.

(16) Pokrzywa, M.; Pawełek, K.; El, W.; Sarbak, S.; Chorell, E.; Almqvist, F.; Wittung-stafshede, P. Effects of Small-Molecule Amyloid Modulators on a Drosophila Model of Parkinson's Disease. *PLoS One* **2017**, *12* (9), 1–21. https://doi.org/10.1371/journal.pone.0184117.

(17) Young, L. M.; Saunders, J. C.; Mahood, R. A.; Revill, C. H.; Foster, R. J.; Tu, L.; Raleigh, D. P.; Radford, S. E.; Ashcroft, A. E. Screening and Classifying Small-Molecule Inhibitors of Amyloid Formation Using Ion Mobility Spectrometry-Mass Spectrometry. *Nat. Chem.* **2015**, *7* (December 2014), 73–81. https://doi.org/10.1038/NCHEM.2129.

(18) Habchi, J.; Chia, S.; Limbocker, R.; Mannini, B.; Ahn, M.; Perni, M.; Hansson, O. Systematic Development of Small Molecules to Inhibit Specific Microscopic Steps of A β 42 Aggregation in Alzheimer ' s Disease. *Proc Natl Acad Sci U S A* **2016**, *114* (2), 200–208. https://doi.org/10.1073/pnas.1615613114.

(19) Joshi, P.; Chia, S.; Habchi, J.; Knowles, T. P. J.; Dobson, C. M.; Vendruscolo, M. A Fragment-Based Method of Creating Small-Molecule Libraries to Target the Aggregation of Intrinsically Disordered Proteins. *ACS Comb. Sci.* **2016**, *18* (3), 144–153. https://doi.org/10.1021/acscombsci.5b00129.

(20) Coelho, T.; Merlini, G.; Bulawa, C. E.; Fleming, J. A.; Judge, D. P. Mechanism of Action and Clinical Application of Tafamidis in Hereditary Transthyretin Amyloidosis. *Neurol. Ther.* **2016**, *5* (1), 1–25. https://doi.org/10.1007/s40120-016-0040-x.

(21) Saunders, J. C.; Young, L. M.; Mahood, R. A.; Jackson, M. P.; Revill, C. H.; Foster, R. J.; Smith, D. A.; Ashcroft, A. E.; Brockwell, D. J.; Radford, S. E. An *in Vivo* Platform for Identifying Inhibitors of Protein Aggregation. *Nat. Chem. Biol.* **2015**, *12* (2), 94–101. https://doi.org/10.1038/nchembio.1988.

(22) Konijnenberg, A.; Ranica, S.; Narkiewicz, J.; Legname, G.; Grandori, R.; Sobott, F.; Natalello, A. Opposite Structural Effects of Epigallocatechin-3-Gallate and Dopamine Binding to A-Synuclein. *Anal. Chem.* **2016**, *88* (17), 6468–6475. https://doi.org/10.1021/acs.analchem.6b00731.

(23) Porat, Y.; Abramowitz, A. Inhibition of Amyloid Fibril Formation by Polyphenols : Structural Similarity and Aromatic Interactions as a Common Inhibition Mechanism. *Chem. Biol. Drg Des.* **2006**, *67* (1), 27–37.

(24) Ono, K.; Yoshiike, Y.; Takashima, A.; Hasegawa, K.; Yamada, M. Potent Anti-Amyloidogenic and Fibril-Destabilizing Effects of Polyphenols *in Vitro* : Implications for the Prevention and Therapeutics of Alzheimer ' s Disease. *Neurochemistry* **2003**, *87* (1), 172–181. https://doi.org/10.1046/j.1471-4159.2003.01976.x.

(25) Townsend, D.; Hughes, E.; Akein, G.; Stewart, K.; Radford, S. E.; Rochester, D.; Middleton, D. A. Epigallocatechin-3-Gallate Remodels Apolipoprotein A-I Amyloid Fibrils into Soluble Oligomers in the Presence of Heparin. *J. Biol. Chem.* **2018**, *17* (33), 12877–12893.

(26) Stefani, M.; Rigacci, S. Beneficial Properties of Natural Phenols : Highlight on Protection against Pathological Conditions Associated with Amyloid Aggregation. *Biofactors* **2014**, *40* (5), 482–493. https://doi.org/10.1002/biof.1171.

(27) Ahmad, E.; Ahmad, A.; Singh, S.; Hameed, A.; Hasan, R. A Mechanistic Approach for Islet Amyloid Polypeptide Aggregation to Develop Anti-Amyloidogenic Agents for Type-2 Diabetes. *Biochimie* **2011**, *93* (5), 793–805. https://doi.org/10.1016/j.biochi.2010.12.012.

(28) Casamenti, F.; Stefani, M. Olive Polyphenols : New Promising Agents to Combat Aging-Associated Neurodegeneration. *Expert Rev. Neurother.* **2017**, *17* (4), 345–358. https://doi.org/10.1080/14737175.2017.1245617.

(29) Wu, C.; Lei, H.; Wang, Z.; Zhang, W.; Duan, Y. Phenol Red Interacts with the Protofibril-Like Oligomers of an Amyloidogenic Hexapeptide NFGAIL through Both Hydrophobic and Aromatic Contacts. *Biophys. J.* **2006**, *91* (10), 3664–3672. https://doi.org/10.1529/biophysj.106.081877.

(30) Hudson, S. A.; Ecroyd, H.; Kee, T. W.; Carver, J. A. The Thioflavin T Fluorescence Assay

for Amyloid Fibril Detection Can Be Biased by the Presence of Exogenous Compounds. *FEBS J.* **2009**, *276* (20), 5960–5972. https://doi.org/10.1111/j.1742-4658.2009.07307.x.

(31) Hasegawa, M.; Smith, M. J.; Goedert, M. Tau Proteins with FTDP-17 Mutations Have a Reduced Ability to Promote Microtubule Assembly. *FEBS Lett.* **1998**, *437*, 207–210. https://doi.org/ 10.1016/s0014-5793(98)01217-4.

(32) Dan, A.; Takahashi, M.; Masuda-suzukake, M.; Kametani, F.; Nonaka, T.; Kondo, H.; Akiyama, H.; Arai, T.; Mann, D. M. A.; Saito, Y.; Hatsuta, H.; Murayama, S.; Hasegawa, M. Extensive Deamidation at Asparagine Residue 279 Accounts for Weak Immunoreactivity of Tau with RD4 Antibody in Alzheimer ' s Disease Brain. *Acta Neuropathol.* **2013**, *279*, 1–9.

(33) Bergen, M. Von; Barghorn, S.; Biernat, J.; Mandelkow, E.; Mandelkow, E. Tau Aggregation Is Driven by a Transition from Random Coil to Beta Sheet Structure. *Biochim. Biophys. Actaand* **2005**, *1739*, 158–166. https://doi.org/10.1016/j.bbadis.2004.09.010.

(34) Micsonai, A.; Wien, F.; Kernya, L.; Lee, Y.; Goto, Y.; Réfrégiers, M.; Kardos, J. Accurate Secondary Structure Prediction and Fold Recognition for Circular Dichroism Spectroscopy. *Proc* **2015**, *112* (24), 3095–3103. https://doi.org/10.1073/pnas.1500851112.

(35) Micsonai, A.; Wien, F.; Bulyáki, É.; Kun, J.; Moussong, É.; Lee, Y.-H.; Goto, Y.; Réfrégiers, M.; Kardos, J. BeStSel: A Web Server for Accurate Protein Secondary Structure Prediction and Fold Recognisiton from the Circular Dichorism Spectra. *Nucleic Acids Res.* **2018**, *46* (W1), W315–W322.

(36) Hussain, R.; Jávorfi, T.; Rudd, T. R.; Siligardi, G. High-Throughput SRCD Using Multi-

Well Plates and Its Applications. *Sci. Rep.* **2016**, *6* (December), 1–6. https://doi.org/10.1038/srep38028.

(37) Soeda, Y.; Yoshikawa, M.; Almeida, O. F. X.; Sumioka, A.; Maeda, S.; Osada, H.; Kondoh, Y.; Saito, A.; Miyasaka, T.; Kimura, T.; Suzuki, M.; Koyama, H.; Yoshiike, Y.; Sugimoto, H.; Ihara, Y.; Takashima, A. Toxic Tau Oligomer Formation Blocked by Capping of Cysteine Residues with 1,2-Dihydroxybenzene Groups. *Nat. Commun.* **2015**, *6*, 1–12. https://doi.org/10.1038/ncomms10216.

(38) Li, J. I. E.; Zhu, M. I. N.; Manning-bog, A. M. Y. B.; Monte, D. A. D. I.; Fink, A. L. Dopamine and L-Dopa Disaggregate Amyloid Fibrils: Implications for Parkinson's and Alzheimer's Disease. *FACEB J.* **2004**, *18* (6), 962–964. https://doi.org/10.1096/fj.03-0770fje.

(39) Liu, M.; Wan, L.; Bin, Y.; Xiang, J. Role of Norepinephrine in A β -Related Neurotoxicity : Dual Interactions with Tyr 10 and SNK (26 – 28) of A β. **2017**, *49* (January), 170–178. https://doi.org/10.1093/abbs/gmw126.

(40) Duynhoven, J. Van; Vaughan, E. E.; Jacobs, D. M.; Kemperman, R. A.; Velzen, E. J. J. Van. Metabolic Fate of Polyphenols in the Human Superorganism. *Proc Natl Acad Sci U S A* **2011**, *108*, 4531–4538. https://doi.org/10.1073/pnas.1000098107.

(41) Rechner, A. R.; Kuhnle, G.; Bremner, P.; Hubbard, G. P.; Moore, K. P.; Rice -Evans, C. A. The Metabolic Fate of Dietary Polyphenols in Humans. *Free Radic. Biol. Med.* **2002**, *33* (2), 220–235.

(42) Rechner, A. R.; Kuhnle, G.; Hu, H.; Roedig-Penman, A.; Van Den Braak, M. H.; Moore, K. P.; Rice-Evans, C. A. The Metabolism of Dietary Polyphenols and the Relevance to

Circulating Levels of Conjugated Metabolites. *Free Radic. Res.* **2002**, *36* (11), 1209–1218. https://doi.org/10.1080/1071576021000016472.

(43) Axelrod, J. O-Methylation of Epinephrine and Other Catechols *in Vitro* and *in Vivo*. *Science (80-.).* **1957**, *126* (3270), 400–401. https://doi.org/10.1126/science.126.3270.400.

(44) Chen, J.; Song, J.; Yuan, P.; Tian, Q.; Ji, Y.; Ren-patterson, R.; Liu, G.; Sei, Y.; Weinberger, D. R. Orientation and Cellular Distribution of Membrane-Bound Catechol- O -Methyltransferase in Cortical Neurons. *J. Biol. Chem.* **2011**, *286* (40), 34752–34760. https://doi.org/10.1074/jbc.M111.262790.

(45) Chen, D.; Drombosky, K. W.; Hou, Z.; Sari, L.; Kashmer, O. M.; Ryder, B. D.; Perez, V. A.; Woodard, D. N. R.; Lin, M. M.; Diamond, M. I.; Joachimiak, L. A. Tau Local Structure Shields an Amyloid-Forming Motif and Controls Aggregation Propensity. *Nat. Commun.* **2019**, *10* (1), 1–14. https://doi.org/10.1038/s41467-019-10355-1.

(46) Sui, D.; Liu, M.; Kuo, M. H. *In Vitro* Aggregation Assays Using Hyperphosphorylated Tau Protein. *J. Vis. Exp.* **2015**, No. 95, 1–9. https://doi.org/10.3791/51537.

(47) Li, H.; Rahimi, F.; Sinha, S.; Maiti, P.; Bitan, G.; Murakami, K. Amyloids and Protein Aggregation-Analytical Methods. In *Encyclopedia of Analytical Chemistry,* **2009**; pp1-32. https://doi.org/10.1002/9780470027318.a9038.

(48) Cohen, S. I. A.; Linse, S.; Luheshi, L. M.; Hellstrand, E.; White, D. A.; Rajah, L.; Otzen, D. E.; Vendruscolo, M.; Dobson, C. M.; Knowles, T. P. J. Proliferation of Amyloid-B42 Aggregates Occurs through a Secondary Nucleation Mechanism. *Proc. Natl. Acad. Sci. U. S. A.* **2013**, *110* (24), 9758–9763. https://doi.org/10.1073/pnas.1218402110.

(49) Caccia, S.; Fong, M. H. Kinetics and Distribution of the B-adrenergic Agonist Salbutamol

in Rat Brain. *J. Pharm. Pharmacol.* **1984**, *36* (3), 200–202. https://doi.org/10.1111/j.2042-7158.1984.tb06941.x.

(50) Jameson, L. P.; Smith, N. W.; Dzyuba, S. V. Dye-Binding Assays for Evaluation of the Effects of Small Molecule Inhibitors on Amyloid (Aβ) Self-Assembly. *ACS Chem. Neurosci.* **2012**, *3* (11), 807–819. https://doi.org/10.1021/cn300076x.

(51) Wishart, D. S.; Feunang, Y. D.; Guo, A. C.; Lo, E. J.; Marcu, A.; Grant, R.; Sajed, T.; Johnson, D.; Li, C.; Sayeeda, Z.; Assempour, N.; Iynkkaran, I.; Liu, Y.; Maciejewski, A.; Gale, N.; Wilson, A.; Chin, L.; Cummings, R.; Le, D.; Pon, A.; Knox, C.; Wilson, M. DrugBank 5 . 0 : A Major Update to the DrugBank Database for 2018. *Nucleic Acids Res.* **2018**, *46* (November 2017), 1074–1082. https://doi.org/10.1093/nar/gkx1037.

(52) Westerhof, F. J.; Zuidhof, A. B.; Kok, L.; Meurs, H.; Zaagsma, J. Effects of Salbutamol and Enantiomers on Allergen-Induced Asthmatic Reactions and Airway Hyperreactivity. *Eur. Respir. J.* **2005**, *25* (5), 864–872. https://doi.org/10.1183/09031936.05.00102203.

(53) Zhang, W.; Falcon, B.; Murzin, A. G.; Fan, J.; Crowther, R. A.; Goedert, M.; Scheres, S. H. W. Heparin-Induced Tau Filaments Are Polymorphic and Differ from Those in Alzheimer's and Pick's Diseases. *Elife* **2019**, *8*, 1–24. https://doi.org/10.7554/eLife.43584.

(54) Méndez, R.; Leplae, R.; Lensink, M. F.; Wodak, S. J. Assessment of CAPRI Predictions in Rounds 3-5 Shows Progress in Docking Procedures. *Proteins Struct. Funct. Genet.* **2005**, *60* (2), 150–169. https://doi.org/10.1002/prot.20551.

(55) Méndez, R.; Leplae, R.; De Maria, L.; Wodak, S. J. Assessment of Blind Predictions of Protein-Protein Interactions: Current Status of Docking Methods. *Proteins Struct. Funct. Genet.* **2003**, *52* (1), 51–67. https://doi.org/10.1002/prot.10393.

(56) Fernández-Recio, J.; Totrov, M.; Abagyan, R. ICM-DISCO Docking by Global Energy Optimization with Fully Flexible Side-Chains. *Proteins Struct. Funct. Genet.* **2003**, *52* (1), 113–117. https://doi.org/10.1002/prot.10383.

(57) An, J.; Totrov, M.; Abagyan, R. Pocketome via Comprehensive Identification and Classification of Ligand Binding Envelopes. *Mol. Cell. Proteomics* **2005**, *4* (6), 752–761. https://doi.org/10.1074/mcp.M400159-MCP200.

(58) Zheng, Q.; Kebede, M. T.; Kemeh, M. M.; Islam, S.; Lee, B.; Bleck, S. D.; Wurfl, L. A.; Lazo, N. D. Inhibition of the Self-Assembly of Aβ and of Tau by Polyphenols: Mechanistic Studies. *Molecules* **2019**, *24* (12), 1–20. https://doi.org/10.3390/molecules24122316.

(59) Wobst, H.; Sharma, A.; Diamond, M.; Wanker, E.; Bieschke, J. The Green Tea Polyphenol (−)-Epigallocatechin Gallate Prevents the Aggregation of Tau Protein into Toxic Oligomers at Substoichiometric Ratios. *FEBS Lett.* **2015**, *589* (1), 77–83. https://doi.org/10.1097/OGX.0000000000000256.Prenatal.

(60) Motamedi-Shad, N.; Monsellier, E.; Chiti, F. Amyloid Formation by the Model Protein Muscle Acylphosphatase Is Accelerated by Heparin and Heparan Sulphate through a Scaffolding-Based Mechanism. *J. Biochem.* **2009**, *146* (6), 805–814. https://doi.org/10.1093/jb/mvp128.

(61) McLaurin, J. A.; Franklin, T.; Zhang, X.; Deng, J.; Fraser, P. E. Interactions of Alzheimer Amyloid-β Peptides with Glycosaminoglycans: Effects on Fibril Nucleation and Growth. *Eur. J. Biochem.* **1999**, *266* (3), 1101–1110. https://doi.org/10.1046/j.1432-1327.1999.00957.x.

(62) Castillo, G. M.; Lukito, W.; Wight, T. N.; Snow, A. D. The Sulfate Moieties of Glycosaminoglycans Are Critical for the Enhancement of β-Amyloid Protein Fibril Formation. *J. Neurochem.* **1999**, *72* (4), 1681–1687. https://doi.org/10.1046/j.1471-4159.1999.721681.x.

(63) Mikawa, S.; Mizuguchi, C.; Nishitsuji, K.; Baba, T.; Shigenaga, A.; Shimanouchi, T.; Sakashita, N.; Otaka, A.; Akaji, K.; Saito, H. Heparin Promotes Fibril Formation by the N-Terminal Fragment of Amyloidogenic Apolipoprotein A-I. *FEBS Lett.* **2016**, *590* (20), 3492–3500. https://doi.org/10.1002/1873-3468.12426.

(64) Goyal, D.; Kaur, A.; Goyal, B. Benzofuran and Indole : Promising Scaffolds for Drug Development in Alzheimer ' s Disease. *Chem Med Chem* **2018**, *13* (13), 1275–1299. https://doi.org/10.1002/cmdc.201800156.

(65) Howlett, D. R.; George, A. R.; Owen, D. E.; Ward, R. V.; Markwell, R. E. Common Structural Features Determine the Effectiveness of Carvedilol, Daunomycin and Rolitetracycline as Inhibitors of Alzheimer β-Amyloid Fibril Formation. *Biochem. J.* **1999**, *343*, 419–423. https://doi.org/10.1038/nbt0994-848c.

(66) Hard, T.; Lendel, C. Inhibition of Amyloid Formation. *J. Mol. Biol.* **2012**, *421* (4–5), 441–465. https://doi.org/10.1016/j.jmb.2011.12.062.

(67) Doig, A. J.; Derreumaux, P. Inhibition of Protein Aggregation and Amyloid Formation by Small Molecules. *Curr. Opin. Struct. Biol.* **2015**, *30*, 50–56. https://doi.org/10.1016/j.sbi.2014.12.004.

(68) Gordonsmith, R. H.; Raxworthy, M. J.; Gulliver, P. A. Substrate Stereospecificity and Selectivity of Catechol-O-Methyltransferase for DOPA, DOPA Derivatives and α-

Substituted Catecholamines. *Biochem. Pharmacol.* **1982**, *31* (3), 433–437. https://doi.org/10.1016/0006-2952(82)90194-0.

(69) Napolitano, A.; Manini, P.; d'Ischia, M. Oxidation Chemistry of Catecholamines and Neuronal Degeneration: An Update. *Curr. Med. Chem.* **2011**, *18* (12), 1832–1845. https://doi.org/10.2174/092986711795496863.

(70) Tsunoda, M.; Uchino, E.; Imai, K.; Takashi, F. Oxidative Stress Increases 6-Nitronorepinephrine and 6-Nitroepinephrine Concentrations in Rat Brain. *Biomed. Chromatogr.* **2008**, *22*, 572–574. https://doi.org/10.1002/bmc.970.

(71) Schmekel, B.; Rydberg, I.; Norlander, B.; Sjöswärd, K. N.; Ahlner, J.; Andersson, R. G. G. Stereoselective Pharmacokinetics of S-Salbutamol after Administration of the Racemate in Healthy Volunteers. *Eur. Respir. J.* **1999**, *13* (6), 1230–1235. https://doi.org/10.1034/j.1399-3003.1999.13f04.x.

(72) Reszka, K. J.; McGraw, D. W.; Britigan, B. E. Peroxidative Metabolism of B2 -Agonists Salbutamol and Fenoterol and Their Analogs. *Chem Res Toxicol* **2009**, *22* (6), 1137–1150. https://doi.org/10.1021/tx900071f.

(73) Green, P. S.; Mendez, A. J.; Jacob, J. S.; Crowley, J. R.; Growdon, W.; Hyman, B. T.; Heinecke, J. W. Neuronal Expression of Myeloperoxidase Is Increased in Alzheimer's Disease. *J. Neurochem.* **2004**, *90* (3), 724–733. https://doi.org/10.1111/j.1471-4159.2004.02527.x.

(74) Gellhaar, S.; Sunnemark, D.; Eriksson, H.; Olson, L.; Galter, D. Myeloperoxidase-Immunoreactive Cells Are Significantly Increased in Brain Areas Affected by Neurodegeneration in Parkinson's and Alzheimer's Disease. *Cell Tissue Res.* **2017**, *369*

(3), 445–454. https://doi.org/10.1007/s00441-017-2626-8.

(75) Uzkeser, H.; Cadirci, E.; Halici, Z.; Odabasoglu, F.; Polat, B.; Yuksel, T. N.; Ozaltin, S.; Atalay, F. Anti-Inflammatory and Antinociceptive Effects of Salbutamol on Acute and Chronic Models of Inflammation in Rats: Involvement of an Antioxidant Mechanism. *Mediators Inflamm.* **2012**, *2012,* 438912. https://doi.org/10.1155/2012/438912.

(76) Kawamura, S.; Yasui, N. Effects of Dobutamine on Brain Surface in Rats. *Neurol Med Chir* **1998**, *38* (3), 141–142.

(77) Ni, Y.; Zhao, X.; Bao, G.; Zou, L.; Teng, L.; Wang, Z.; Song, M.; Xiong, J. Activation of B2 -Adrenergic Receptor Stimulates γ-Secretase Activity and Accelerates Amyloid Plaque Formation. *Nat. Med.* **2006**, *12* (12), 1390–1396. https://doi.org/10.1038/nm1485.

(78) Chai, G. S.; Wang, Y. Y.; Yasheng, A.; Zhao, P. Beta 2-Adrenergic Receptor Activation Enhances Neurogenesis in Alzheimer's Disease Mice. *Neural Regen. Res.* **2016**, *11* (10), 1617–1624. https://doi.org/10.4103/1673-5374.193241.

(79) Eschmann, N. A.; Georgieva, E. R.; Ganguly, P.; Borbat, P. P.; Rappaport, M. D.; Akdogan, Y.; Freed, J. H.; Shea, J. E.; Han, S. Signature of an Aggregation-Prone Conformation of Tau. *Sci. Rep.* **2017**, *7*, 1–10. https://doi.org/10.1038/srep44739.

(80) Von Bergen, M.; Friedhoff, P.; Biernat, J.; Heberle, J.; Mandelkow, E. M.; Mandelkow, E. Assembly of τ Protein into Alzheimer Paired Helical Filaments Depends on a Local Sequence Motif (306-VQIVYK-311) Forming β Structure. *Proc. Natl. Acad. Sci. U. S. A.* **2000**, *97* (10), 5129–5134. https://doi.org/10.1073/pnas.97.10.5129.

For Table of Contents Only